DE GRUYTER Pure Appl. Chem. 2020; 92(3): 493–503

Conference paper

Réka Henyecz, Zoltán Mucsi and György Keglevich*

A surprising mechanism lacking the Ni(0) state during the Ni(II)-catalyzed P–C cross-coupling reaction performed in the absence of a reducing agent – An experimental and a theoretical study

https://doi.org/10.1515/pac-2019-1004

Abstract: The Hirao reaction, i.e. the P–C coupling between a bromoarene and a >P(O)H reagent performed in most cases in the presence of a Pd(0) complex incorporating a *P*-ligand may also be carried out applying a Ni(II) catalyst precursor with or without Zn or Mg as the reducing agent. The Ni catalysts may include *P*- or *N*-ligands. B3LYP/6-31G(d,p)//PCM(MeCN) quantum chemical calculations suggested that the mechanism of the NiX$_2$ catalyzed (X=Cl or Br) P–C couplings performed in the absence of a reducing agent, and in the excess of the >P(O)H reagent serving as the *P*-ligand (via its tautomeric >POH form) is completely different from that of the Pd(OAc)$_2$ promoted version, as no reduction of the Ni(II) occurs. In the two variations mentioned, the active catalyst is the dehydrobrominated species derived from primary complex [(HO)Y$_2$P]$_2$Ni(II)Br$_2$, and the [(HO)Y$_2$P]$_2$Pd(0) complex itself, respectively. Both species undergo temporary oxidation (to "Ni(IV)" and "Pd(II)", respectively) in the catalytic cycle. During the catalysis with "P$_2$Ni(II)X$_2$", one of the *P*-ligands serves the >P(O)H function of the ArP(O)H< product. The consequence of this difference is that in the Ni(II)-catalyzed case, somewhat less >P(O)H-species is needed than in the Pd(0)-promoted instance. Applying 10 % of the Pd(OAc)$_2$ or NiX$_2$ precursor, the optimum quantity of the *P*-reagent is 1.3 equivalent and, in the first approach, 1.1 equivalent, respectively. Preparative experiments justified the new mechanism explored. The ligation of Ni(II) was also investigated by theoretical calculations. It was proved that the bis-complexation is the most favorable energetically as compared to the mono-, tri- and tetra-ligation.

Keywords: cross coupling; ICPC-22; microwave heating; nickel(II) catalyst; *P*-ligands; quantum chemistry; reaction mechanisms.

Introduction

The Hirao reaction involving the P–C coupling of aryl or vinyl halides and >P(O)H reagents is a useful synthetic technique for the preparation of phosphonates, phosphinates and tertiary phosphine oxides [1–4]. Originally tetrakis(triphenylphosphine)palladium was applied as the catalyst, then different Pd(0) precursors including Pd(II) salts were utilized together with triphenylphosphine, or bidentate *P*-ligands [3, 4]. There is an agreement that in all cases the "*ab ovo*" present, or initially formed Pd(0) undergoes oxidative addition with the, let say, aryl halide that is followed by ligand exchange by the >P(O)H species. The catalytic cycle ends up with a reductive elimination to afford the phosphonate or phosphine oxide, and regenerate

---

Article note: A collection of invited papers based on presentations at the 22nd International Conference on Phosphorous Chemistry (ICPC-22) held in Budapest, Hungary, 8–13 July 2018.

***Corresponding author: György Keglevich,** Department of Organic Chemistry and Technology, Budapest University of Technology and Economics, 1521 Budapest, Hungary, e-mail: gkeglevich@mail.bme.hu
Réka Henyecz and Zoltán Mucsi: Department of Organic Chemistry and Technology, Budapest University of Technology and Economics, 1521 Budapest, Hungary

the Pd(0) catalyst [5–7]. We found that there is no need to apply mono- or bidentate *P*-ligands together with the Pd(OAc)$_2$ catalyst, as the excess of the >P(O)H reagent may serve as the complexing agent in its trivalent (>POH) form. Moreover, the >P(O)H species may also act as the reductant [8–10]. The classical mechanism of the Hirao reaction was refined for the case, when no commercial *P*-ligands were added, and the excess of the diethyl phosphite or diphenylphosphine oxide reagents served as the *P*-ligand [10]. Recently, the formation of the (HO)Y$_2$P···Pd(0)···PY$_2$(OH) catalyst was explored in detail, and it was found that the Pd(0) complex displays an enhanced reactivity if the *P*-ligands contain 2-MeC$_6$H$_4$ or 3-MeC$_6$H$_4$ aryl groups causing sterical hindrance, as compared to the presence of the phenyl group [11]. This is the consequence of the energetically preferred bis-ligation with suppressed tris-ligation, when the Ar$_2$POH ligands with the 2-MeC$_6$H$_4$ or 3-MeC$_6$H$_4$ groups are present.

The Ni-catalyzed Hirao reactions form a less studied, but interesting field. A part of the P–C couplings were performed using Ni(II) salts together with Zn or Mg as the reducing agent to form Ni(0) [12–19]. In a part of the cases *P*-ligands [12, 19], in other instances *N*-ligands [13–19] were used to form the Ni complexes. The theoretical calculations [18] of Zhao and co-workers justified the involvement of Ni(0) in the usual catalytic cycle starting with oxidative addition of the, in this case, vinyl bromide reactant. This protocol is analogous to the Pd(0)-catalyzed cycle [10].

A series of aryl/vinyl boronates/iodides/sulfonates/nitriles were reacted with secondary phosphine oxides or dialkyl phosphites in the presence of Ni(II) salts, Ni(acac)$_2$ or Ni(COD)$_2$ together with mono- or bidentate *N*-ligands [20–23]. Mono- and bidentate *P*-ligands, such as PPh$_3$, PCy$_3$, or dppp, dppe, dppf, dppb, dcype and BINAP, respectively, were also applied together with NiCl$_2$ or Ni(COD)$_2$ [24–35]. When applying the Ni(acac)$_2$ and Ni(COD)$_2$ precursors, principally, the classical mechanism [13, 18, 19, 34–36] may work, however, the way of operation of Ni(II) salts in the absence of reductants is uncertain. In a special case, CeO$_2$- or Al$_2$O$_3$-based Ni-nanoparticles were used in the P–C coupling of aryl halides and secondary phosphine oxides [37]. We elaborated a microwave (MW)-assisted protocol, in which the excess of the >P(O)H reagents served as the *P*-ligand for the NiCl$_2$ catalyst precursor [38]. This method seemed to be of general value.

It was a challenge for us to evaluate the mechanism of the NiX$_2$-catalyzed (X=Cl or Br) P–C coupling on the simple model reaction of bromobenzene with diphenylphosphine oxide and diethyl phosphite carried out in the absence of a reducing agent using the excess of the >P(O)H reagent as the *P*-ligand.

Results and discussion

Optimization of the NiX$_2$-catalyzed Hirao reaction of >P(O)H reagents with bromobenzene

First, we wished to optimize the P–C coupling reaction of bromobenzene with diphenylphosphine oxide in acetonitrile applying 10 % of NiCl$_2$ as the catalyst, and Cs$_2$CO$_3$ as the base under MW irradiation (Scheme 1). We aimed at determining the optimum quantity of diphenylphosphine oxide for the reaction performed

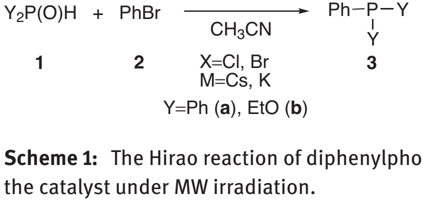

Scheme 1: The Hirao reaction of diphenylphosphine oxide and diethyl phosphite with bromobenzene in the presence of NiX$_2$ as the catalyst under MW irradiation.

at 150 °C for 20 min in acetonitrile. On the analogy of our earlier experiences with $Pd(OAc)_2$ [10] it was expected that one equivalent of the >P(O)H species to the catalyst might ensure the Ni(II)→Ni(0) reduction, while two equivalents would serve the *P*-ligand *via* the trivalent tautomeric form >POH. Applying diphenylphosphine oxide in quantities of 1.0, 1.1, 1.2, and 1.3 equivalents, triphenylphosphine oxide (**3a**) was obtained in yields of 66 %, 76 %, 79 %, and 65 %, respectively (Table 1/Entries 1–4). A similar trend was observed, when $NiBr_2$ was used instead of $NiCl_2$, however, in these cases, the yields of product **3a** were somewhat lower (Table 1/Entries 5–8). In our case, $NiCl_2$ seemed to be the choice of catalyst precursor. Without going into details, applying diethyl phosphite as the *P*-reagent, again a quantity of 1.2 equivalents proved to be optimal. In this case, a reaction temperature of 150 °C, and a time of 45 min was found to be the most advantageous, and the application of K_2CO_3 instead of Cs_2CO_3 led to better results (Table 1/Entries 9 and 10). Among the different experiments performed, the best combination is the P–C coupling of PhBr and $Ph_2P(O)H$ carried out in the presence of $NiCl_2$ and Cs_2CO_3 (Table 1/Entry 3). It was also proved that MW-assistance is inevitable, as the control experiments of the $Ph_2P(O)H$ + PhBr reaction carried out on conventional heating, but otherwise under similar conditions took place in low conversion allowing yields of 36/25 % (Table 1/Entries 11 and 12). Our experiments suggested that in function of the quantity of the *P*-reagent, the yields followed a curve going through a maximum, and that the optimum quantity of diphenylphosphine oxide was 1.2 equivalents. Using less of the reagent was not enough, while measuring it in an excess made the preparation (i.e. the purification *via* chromatography) somewhat inefficient. However, it is worthy to mention that the difference between the outcome of the P–C couplings applying 1.1 or 1.2 equivalents of the $Ph_2P(O)H$ reagent is not significant (Table 1/Entry 2 vs. 3 and Entry 6 vs. 7). The need, in the first approach, for only 1.2 equivalents of the >P(O)H species may substantiate that in the NiX_2-catalyzed Hirao reactions studied by us, Ni(II) is not reduced by the >P(O)H reagent, and a catalyst of $[(HO)Y_2P]_2NiX_2$ type may be formed. It is recalled that in the P–C couplings elaborated by Zhao *et al.* and others using Zn or Mg as the reducing agent, and bipyridyl as an *N*-ligand, certainly Ni(0) was the catalyst [13–19]. To clarify the situation for our case, we wished to evaluate the mechanism of the Hirao reaction performed in the absence of a reducing agent, using NiX_2 (X=Cl or Br) as the catalyst precursor and some excess of the >P(O)H reagent as the *P*-ligand.

Table 1: Optimization of the MW-assisted P–C coupling reaction of $Y_2P(O)H$ reagents with bromobenzene applying NiX_2 catalyst in acetonitrile at 150 °C.

$Y_2P(O)H$		NiX_2 (10 %)	Base (1 equiv.)	Time (min)	Conversion (%)[a]	Isolated yield (%)[b]	Entry
Y	Quantity (equiv.)						
Ph	1.0	$NiCl_2$	Cs_2CO_3	20	100	66 (**3a**)	1
Ph	1.1	$NiCl_2$	Cs_2CO_3	20	100	76 (**3a**)	2
Ph	1.2	$NiCl_2$	Cs_2CO_3	20	100	79 (**3a**)	3
Ph	1.3	$NiCl_2$	Cs_2CO_3	20	100[c]	65 (**3a**)	4
Ph	1.0	$NiBr_2$	Cs_2CO_3	30	100	55 (**3a**)	5
Ph	1.1	$NiBr_2$	Cs_2CO_3	30	100	69 (**3a**)	6
Ph	1.2	$NiBr_2$	Cs_2CO_3	30	100	72 (**3a**)	7
Ph	1.3	$NiBr_2$	Cs_2CO_3	30	100[c]	55 (**3a**)	8
EtO	1.2	$NiCl_2$	K_2CO_3	45	~90	70 (**3b**)	9
EtO	1.2	$NiBr_2$	K_2CO_3	45	~90	65 (**3b**)	10
Ph[d]	1.2	$NiCl_2$	Cs_2CO_3	20	65	36 (**3a**)	11
Ph[d]	1.2	$NiBr_2$	Cs_2CO_3	30	69	25 (**3a**)	12

[a] Based on relative ^{31}P NMR intensities.
[b] The average of 3 parallel measurements.
[c] $Ph_2P(O)H$ remained in the reaction mixture.
[d] Comparative thermal experiment.

Theoretical calculations

A study on the ligation of nickel(II)

The calculations on the complexation of Ni(II) with the trivalent tautomeric form (Y_2POH) of diphenylphosphine oxide and diethyl phosphite applying $NiCl_2$ or $NiBr_2$ were carried out at the B3LYP level of theory using the 6-31G(d,p) basis set including the explicit-implicit solvent model (Scheme 2) [39–42]. Earlier, this approach proved to be suitable to describe adequately the reactions studied [10, 11]. The limiting factor for the basis set was the large size of a few Ni complexes. In the discussion, we rely rather on the calculated enthalpy values (*H*) instead of Gibbs free energies (*G*) due to the significant uncertainty of the calculated entropy values (*S*) of such large complexes. The enthalpy values for the complexations are listed in Table 2, and shown in Fig. 1. It was found that the mono- (**4**) and bis-ligated Ni(II) complexes (**5**) are formed in exothermic reactions for both cases (Y=Ph and EtO) studied. The ligation is preceded by an endothermic tautomerization of the pentavalent $Y_2P(O)H$ to the trivalent Y_2POH characterized by 22.9 kJ mol^{-1} (Y=Ph) and 25.1 kJ mol^{-1} (Y=OEt). In the following part, all enthalpies are given relative to the more stable $Y_2P(O)H$ form. The mono-ligation with Ph_2POH and $(EtO)_2POH$ is characterized by delta enthalpy values of –243.7(Cl)/–333.7(Br) kJ mol^{-1}, and –216.7(Cl)/ – 303.3(Br) kJ mol^{-1}, respectively, while the similar numbers for bis-ligation are –81.4(Cl)/–96.8(Br) kJ mol^{-1}, and –64.2(Cl)/ – 83.0(Br) kJ mol^{-1}, respectively. The tris-complexation (to give species **6**) is not favorable, and turned to endothermic in both cases. For Ph_2POH and $(EtO)_2POH$, these values are 34.1(Cl)/100.2(Br) kJ mol^{-1}, and 69.3(Cl)/137.0(Br) kJ mol^{-1}, respectively. The tetra-ligation (leading to **7**) is even more unfavorable for the Ph_2POH ligand, obviously as a consequence of steric hindrance, and characterized by larger enthalpy values of 108.6(Cl)/183.8(Br) kJ mol^{-1}. At the same time, for the $(EtO)_2POH$ ligand, the enthalpy values of the tetra-ligation [41.1(Cl)/115.0(Br) kJ mol^{-1}] are comparable with those of the tris-ligation [69.3(Cl)/137.0(Br) kJ mol^{-1}]. The gross energetics can be seen in Fig. 1/**a1–b1** (Y=Ph) and **a2–b2** (Y=EtO). Bis-ligated complex **5** may undergo deprotonation, and then loss of X^- to afford species **8** and **9**, respectively. At the same time, the proton loss of complexes **6** and **7** furnishes forms **10** and **11**, respectively. It is noted that the complexation degree of a catalyst is a crucial parameter during the reaction it is involved in. An "under-complexed" metal (as in **4**) is not active and not stabilized sufficiently. At the same time, an overcrowded complex like species **6** and **7** surrounded by more ligands deactivates the catalyst, hence preventing its assistance in the reaction, where it is involved. From among the species discussed, **5** may

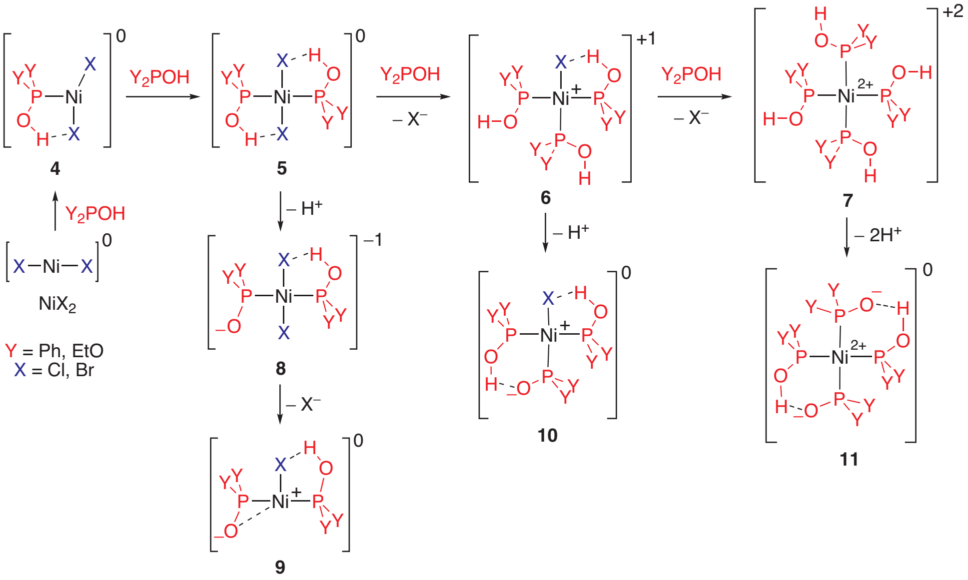

Scheme 2: Ligation of NiX_2 with Y_2POH.

Table 2: The computed complexation and deprotonation enthalpies (Δ*H*) and Gibbs free energies (Δ*G*) in kJ mol⁻¹ for $NiCl_2$ and $NiBr_2$ with Ph_2POH and $(EtO)_2POH$ ligands at B3LYP/6-31G(d,p)//PCM(MeCN) level of theory.

	Y=Ph				Y=OEt			
	$X=Cl^-$		$X=Br^-$		$X=Cl^-$		$X=Br^-$	
	Δ*H* (kJ mol⁻¹)	Δ*G* (kJ mol⁻¹)	Δ*H* (kJ mol⁻¹)	Δ*G* (kJ mol⁻¹)	Δ*H* (kJ mol⁻¹)	Δ*G* (kJ mol⁻¹)	Δ*H* (kJ mol⁻¹)	Δ*G* (kJ mol⁻¹)
NiX_2→4	−243.7	−199.5	−333.7	−273.1	−216.7	−172.7	−303.3	−253.5
4→5	−81.4	−29.4	−96.8	−51.1	−64.2	−15.7	−83.0	−26.1
5→6	34.1	69.8	100.2	137.8	69.3	98.2	137.0	161.0
6→7	108.8	152.3	183.8	205.1	41.1	60.1	115.0	132.8
5→8	−133.2	−131.9	−131.9	−132.4	−171.4	−160.7	−161.8	−163.1
8→9	−0.9	−40.5	75.9	40.7	53.7	9.8	121.5	90.1
6→10	−103.1	−110.5	−96.2	−102.6	−115.1	−122.6	−128.6	−141.7
7→11	−476.7	−485.8	−476.7	−485.8	−421.3	−418.1	−421.3	−418.1

The reaction steps are illustrated in Scheme 2.

be the best catalyst, while **6** and **7** are hindered forms. Deprotonation of the complexes (**5–7**) is highly favorable. It is noteworthy that there is a considerable difference between the enthalpies of the dissociation of the bromo- and chloro-containing species **8**. The dissociation of the bromo anion from **8** is much more unfavorable than that of the chloro anion, suggesting a stronger Ni(II)–Br bonding as compared to the Ni(II)–Cl connection. This dissociation step has an important role on the overall reactivity of the NiX_2 species applied (see later).

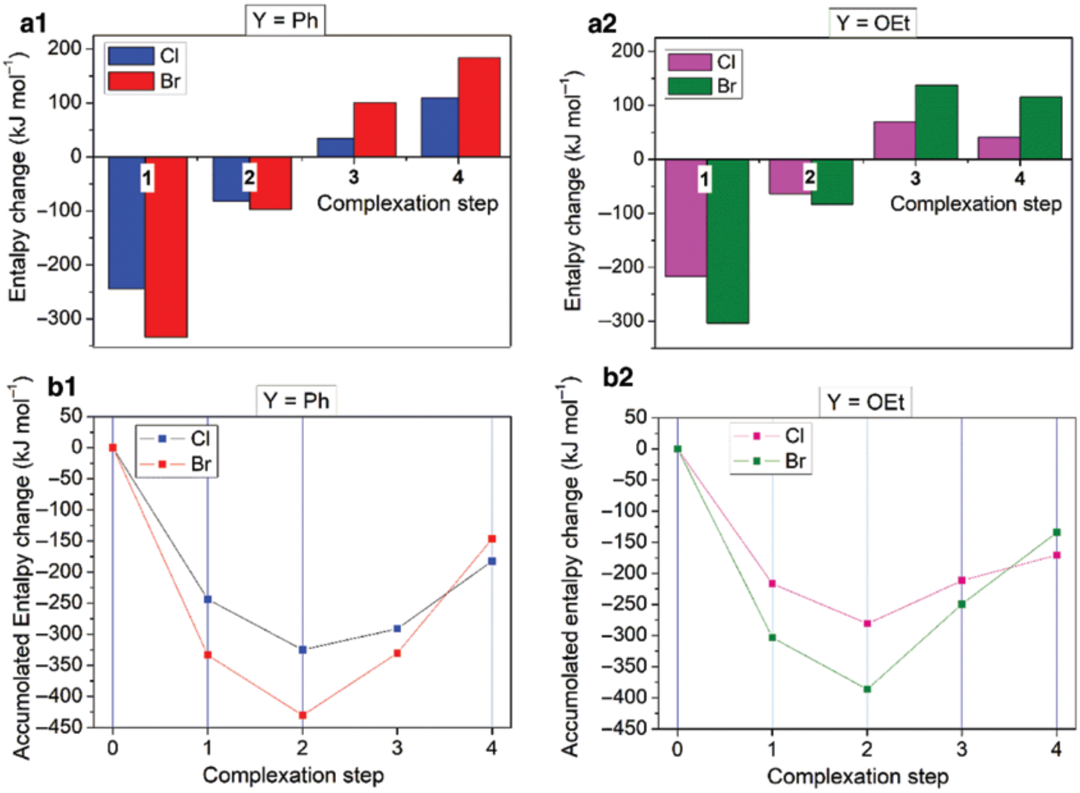

Fig. 1: Enthalpy changes (**a1** and **a2**) and total enthalpy changes (**b1** and **b2**) in kJ mol⁻¹ for the mono-, bis-, tris- and tetra-ligation of $NiCl_2$ and $NiBr_2$ with Ph_2POH and $(EtO)_2POH$ ligands computed by the B3LYP/6-31G(d,p)//PCM(MeCN) method.

The mechanism of the Ni(II)-catalyzed Hirao reaction

According to the calculations by the B3LYP/6-31G(d,p)//PCM(MeCN) method, the catalytic cycle can be divided into three main stages, such as the catalyst preactivation, insertion into the C–Br bond (oxidative addition), and formation of the C–P bond (reductive elimination) (Scheme 3; for the Δ*H* and Δ*G* values see Table 3). For clarity, $NiBr_2$ was considered as the catalyst precursor to match the PhBr substrate. Species **15** is the reactive Ni(II) complex that is formed from initial complex **13** by deprotonation, and by the loss of a bromide anion. Form **15** may be bound loosely *via* its Ni(II) center to the bromo atom of PhBr (**2**) forming reagent-catalyst complex **16.** In the next step, the second bromide anion is also leaving to provide an intermediate (**17**) stabilized by a strong internal *H*-bond. It is noted that assuming the chloro analogue complex of **16** that is **16***

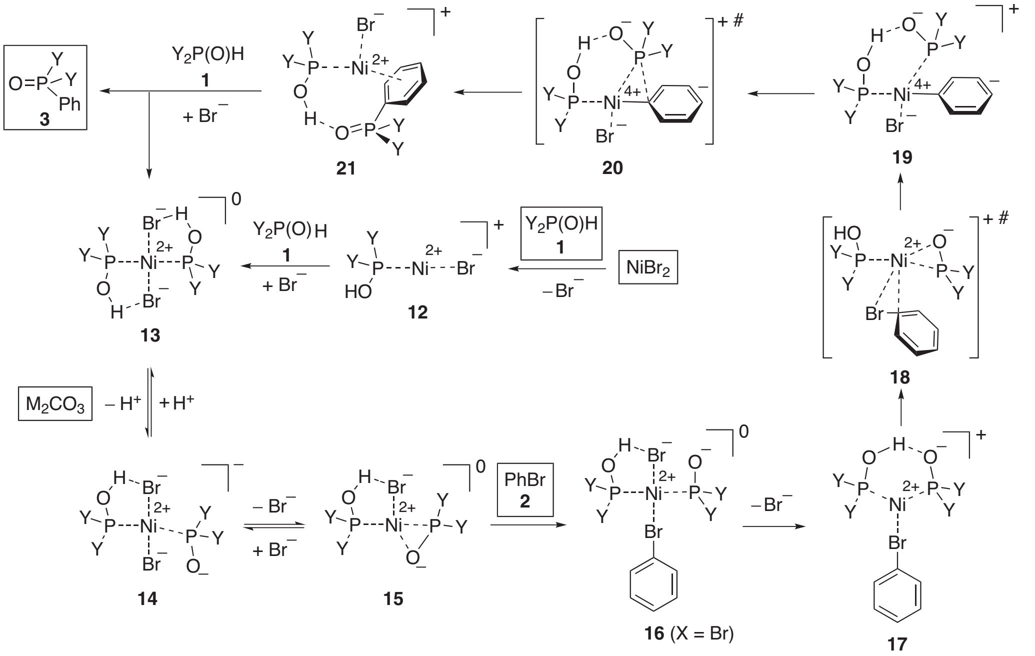

Scheme 3: The mechanism of the $NiBr_2$-catalyzed Hirao reaction of PhBr and $Y_2P(O)H$ reagents (Y=Ph or EtO) assuming the later also as the *P*-ligand. The B3LYP/6-31G(d,p)//PCM(MeCN) method was applied.

Table 3: Enthalpy (Δ*H*) and Gibbs free energy (Δ*G*) changes in kJ mol⁻¹ during the mechanism computed for the reaction of PhBr with $(EtO)_2P(O)H$ or $Ph_2P(O)H$ in the presence of $NiBr_2$ (or $NiCl_2$) by the B3LYP/6-31G(d,p)//PCM(MeCN) level of theory with the explicit–implicit solvent model.

	Y=Ph		Y=EtO	
	Δ*H* (kJ mol⁻¹)	**Δ*G* (kJ mol⁻¹)**	**Δ*H* (kJ mol⁻¹)**	**Δ*G* (kJ mol⁻¹)**
13	0.0	0.0	0.0	0.0
14	−131.9 (−131.9)	−132.4 (−134.4)	−153.3 (−180.2)	−154.1 (−181.5)
15	−55.9 (−134.1)	−91.7 (−40.5)	−43.0 (−126.0)	−79.8 (−162.5)
16	−104.9 (−175.4)	−60.9 (−7.5)	−133.4 (−212.1)	−120.2 (−196.5)
17	64.3 (−77.3)	52.5 (44.8)	55.4 (−86.2)	33.3 (−108.3)
18	99.3 (−42.3)	97.5 (85.0)	95.4 (−46.2)	33.4 (−108.4)
19	43.1 (−98.5)	41.2 (73.7)	73.2 (−68.4)	−7.1 (−148.7)
20	77.6 (−64.0)	78.4 (−111.0)	102.1 (−39.5)	105.2 (−36.4)
21	−39.7 (−181.3)	−38.5 (−176.7)	−58.2 (−199.8)	−102.8 (−244.4)
13+3	−225.2 (−366.8)	−206.2 (−342.8)	−273.1 (−414.7)	−259.8 (−401.4)

(deriving from the initial use of $NiCl_2$), its dissociation to species **17** is more favorable, as the enthalpy level of **16*** is by 78.8 kJ mol^{-1} higher than that of **16** making the catalytic cycle more efficient for $NiCl_2$. Another remark is that for clarity, TSs with low barriers of <10 kJ mol^{-1} (e.g. deprotonation, dissociation, or addition starting from species **13–17**) not determining significantly the reaction profile, were not given in Scheme 3 and Fig. 2.

Then, the phenyl group migrates to the Ni moiety to afford complex **19** *via* transition state **18**. In this oxidative addition step, the central Ni(II) is oxidized to Ni(IV). An analogous Ni(II)→Ni(IV) conversion was observed during a $Ni(OTs)_2/PPh_3$-catalyzed C_{Ar}-alkylation [43]. Finally, the new P–C bond is formed *via* transition state **20** *via* reductive elimination yielding the final product (**3**) as its η^6–Ni(II) complex (**21**). The interaction of this complex (**21**) with a molecule of the reagent (**1**) and a bromide anion regenerates catalyst **13**, and affords free product **3**. It can be seen that during the **13**→**21** conversion, one of the >POH ligands in the $[(HO)Y_2P]_2Ni(II)$ complex is consumed to serve the $-P(O)Y_2$ function of the Hirao product (**3**). According to this, if 10 % of NiX_2 is applied, theoretically 1.1 equivalents of the >P(O)H species would be needed to provide the complex of the product (**21**). However, as can be seen from the experimental data (Table 1/Entries 2–3 and 6–7), the use of 1.2 equivalents of the *P*-reagent is better as gives the free product (**3**), and allows the regeneration of the Ni(II) complex (**13**) after the catalytic cycles.

The enthalpy diagram showing the curves for the Hirao reaction of PhBr with $Ph_2P(O)H$ and $(EtO)_2P(O)H$ are shown in Fig. 2. Comparing the Ph- and EtO-substituted cases, one can see that they exhibit analogous enthalpy curves. The only remarkable difference is that the second transition state (**20**) is of lower enthalpy for the Ph-substituted case, than for the EtO-substituted variation. This slight energy difference may explain the somewhat enhanced reactivity of $Ph_2P(O)H$.

It is noteworthy that applying $NiCl_2$ as the catalyst precursor, the enthalpy value for the formation of intermediate **17** from **16** is reasonably lower, as compared to the case using $NiBr_2$. This is marked by 98.1 (Y=Ph, X=Cl) and 125.9 (Y=EtO, X=Cl) kJ mol^{-1}, versus 169.2 (Y=Ph, X=Br) and 188.8 (Y=EtO, X=Br) kJ mol^{-1}, respectively (see Figs. 2 and 3, as well as Figure/Supplementary Info as the superposition of the curves of Figs. 1 and 2). The energy barrier of the subsequent transition state (**18**) represent a relatively low value (35.0 kJ mol^{-1} for Y=Ph, and 41.0 kJ mol^{-1} for Y=OEt). Sure enough, the preparative experiments were more efficient with $NiCl_2$ (see Entries 3 and 7 of Table 1). The enthalpy requirement of 133.1–165.9 kJ mol^{-1} for **16**→**18**

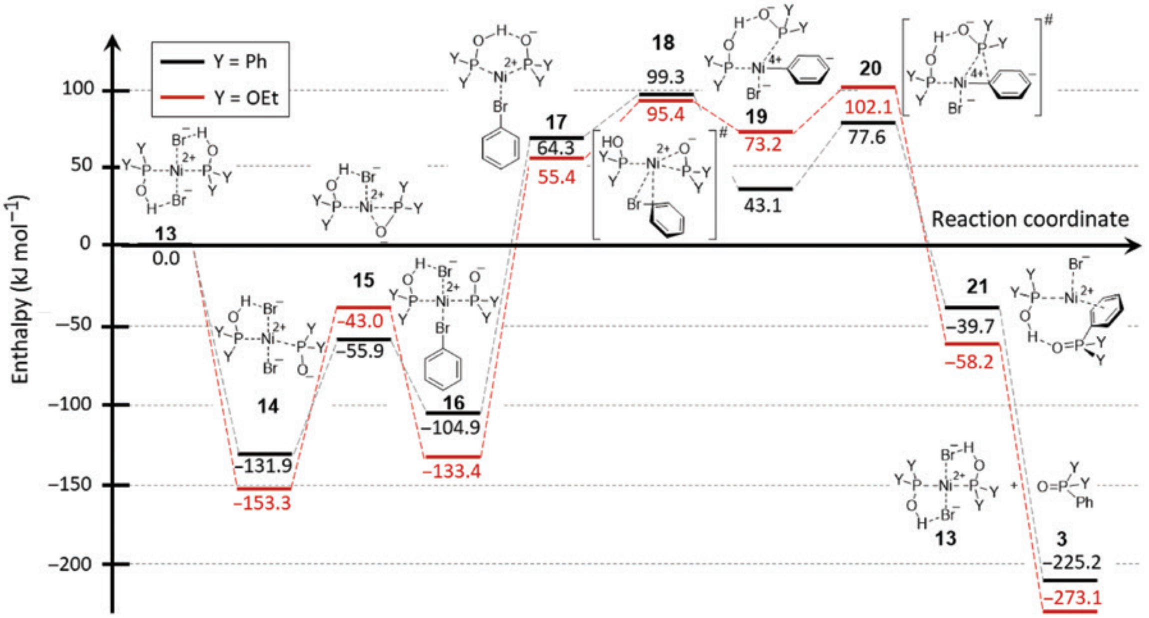

Fig. 2: Enthalpy diagram for the P–C coupling reaction of PhBr with $(EtO)_2P(O)H$ or $Ph_2P(O)H$ in the presence of $NiBr_2$ as the catalyst precursor computed by the B3LYP/6-31G(d,p)//PCM(MeCN).

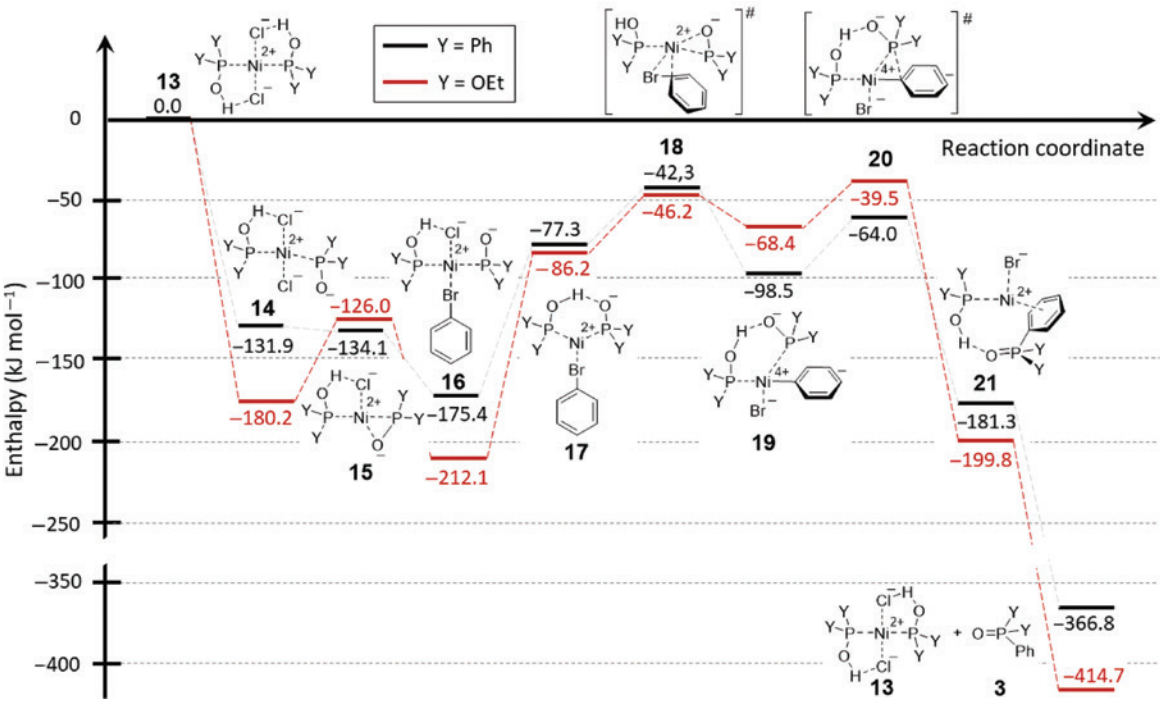

Fig. 3: Enthalpy diagram for the P–C coupling reaction of PhBr with $(EtO)_2P(O)H$ or $Ph_2P(O)H$ in the presence of $NiCl_2$ as the catalyst precursor computed by the B3LYP/6-31G(d,p)//PCM(MeCN).

using $NiCl_2$ as the catalyst precursor may be overcome by MW irradiation. It was found earlier that the direct esterification of P-acids characterized by $\Delta H^{\#}$ values of 135–186 kJ mol^{-1} can be performed under MWs [44, 45]. The enhancing effect is due to the statistically occurring local overheatings (that may be between 1 and 60 °C) in the bulk of the reaction mixture [46–48]. At the same time, the barriers of 204.2–228.8 kJ mol^{-1} calculated for the $NiBr_2$-catalyzed case is at the limit that is manifested in the somewhat lower efficiency of these reactions (see Table 1/Entry 7).

Finally, it is worth comparing the mechanism of the Pd(0)-catalyzed Hirao reaction described by us earlier [10] with that proposed above for Ni(II) catalysis. Both mechanisms comprise the metal insertion into the C–Br bond, and the formation of the P–C bond as the key steps, however, the realization regarding the elementary steps is different. Regarding the metal insertion, the overall activation enthalpy proved to be much lower for the case with Pd(0) (55.8 kJ mol^{-1} for Y=Ph and 58.5 kJ mol^{-1} for Y=OEt) [10] than that for Ni(II) (regarding the **16**→**18** transformation 204.2 kJ mol^{-1} for Y=Ph and 228.8 kJ mol^{-1} for Y=EtO) resulting in a much slower rate for the metal insertion into the C–Br bond in the latter instance. It is noted that the consideration of $NiCl_2$ instead of $NiBr_2$ in the calculations led to lower activation enthalpies (such as 133.1 kJ mol^{-1} for Y=Ph and 165.9 kJ mol^{-1} for Y=EtO). The P–C bond formation exhibits a higher activation barrier with Pd(0) (98.5 kJ mol^{-1} for Y=Ph and 76.6 kJ mol^{-1} for Y=OEt) [10] than with Ni(II) (in respect of the **19**→**20** conversion 34.5 kJ mol^{-1} for Y=Ph and 28.9 kJ mol^{-1} for Y=OEt). According to the above data, Pd(0) can split the C–Br bond much easier than Ni(II), while the product formation is somewhat more favorable in the case of Ni(II) catalysis. Considering that Pd(0) may be nearly equally involved in bis- and tris-ligation [11], and the preference for Ni(II) is the catalytically active bis-ligation, the more beneficial complexation equilibrium for Ni(II) may provide a higher concentration of the $[(HO)Y_2P]_2Ni(II)Br_2$ catalyst precursor and the species derived from it, somewhat compensating the reluctant C–Br fission in the case under discussion.

It is noteworthy that in the Ni(II)-catalyzed Hirao reactions investigated, the >P(O)H species cannot act as a reducing agent. This was checked in separate experiments irradiating the mixture of $NiCl_2$ and $Ph_2P(O)H$ or $(EtO)_2P(O)H$ (the former in acetonitrile solution) at 150 °C for 20 min or 45 min, respectively. On workup, the >P(O)H reagents were regenerated unchanged as suggested by the ^{31}P NMR chemical shifts and LC-MS.

The ability of $Ph_2P(O)H$ to reduce Ni(II) to Ni(0) was also investigated by pre-calculations. Preliminary [B3LYP/6-31G(d,p)] calculations performed on the $Ni(II)(PPh_2OH)_2 \rightarrow Ni(0)(PPh_2OH)_2$ conversion by $Ph_2P(O)H$ in EtOH as solvent suggested an unfavorable endothermic reaction. As a comparison, the earlier reported reduction of Ni(II) by Mg(0) in the presence of 2-,2′-bipyridyl ligand [13–19] exhibited a strongly exothermic transformation.

Conclusions

It was found that the MW-assisted NiX_2-catalyzed (X=Cl or Br) Hirao reaction of bromobenzene and diphenylphosphine oxide or diethyl phosphite took place in the presence of some excess of the >P(O)H reagent acting as the *P*-ligand via its tautomeric >POH form. $NiCl_2$ was found more efficient as the catalyst precursor than $NiBr_2$. Applying 10 % of the NiX_2 precursor, the optimum quantity of the *P*-reagent is 1.2 equivalent. Surprisingly, the P–C coupling took place in the absence of a reducing agent, like Zn or Mg that was needed in a part of the earlier cases. Quantum chemical calculations suggested that the real catalyst is surprisingly a Ni(II) complex formed by dehydrobromination from primary complex $[(HO)Y_2P]_2Ni(II)Br_2$. In the catalytic cycle, one of the *P*-ligands serves the >P(O)H function of the ArP(O)H< product. The protocol with $NiCl_2$ goes with lower enthalpy of activation than that with $NiBr_2$. The involvement of this type of “$Ni(II)P_2$” complex was also justified by calculations on the energetics of the mono-, bis-, tris- and tetra-ligation of the Ni^{2+} ion. Preparative experiments suggested the need for two equivalents of the >P(O)H species to provide the two *P*-ligands for the NiX_2 catalyst precursor. Detailed mechanisms were proposed for the formation of the $[(HO)Y_2P]_2Ni(II)Br_2$ catalyst precursor and the species derived from it, and for the brand new Ni(0)-free protocol of the Hirao reaction. According to this, no reduction of the Ni(II) to Ni(0), but an oxidative addition of the >POH species to afford a Ni(IV) intermediate occurred. Experimental data were in full accord with the theory. Although this theoretical study was limited only to two simple model reactions, earlier experiences [9] confirmed that the NiX_2-promoted P–C coupling between aryl bromides and >P(O)H reagents is of general value.

Experimental

General information

The chemicals used in this study were of a purity >98 % and purchased from Aldrich. The reactions were carried out in a 300 W CEM® Discover (CEM Microwave Technology Ltd., Buckingham, UK) type focused microwave reactor equipped with a stirrer and a pressure controller applying 30–100 W irradiation under isothermal conditions. The reaction mixtures were irradiated in sealed glass vessels (with a volume of 10 mL) available from the supplier of CEM®. The reaction temperature was monitored by an external IR sensor.

The ^{31}P, ^{13}C and ^{1}H NMR spectra were obtained in $CDCl_3$ solution on a Bruker AV-300 spectrometer operating at 121.5, 75.5 and 300 MHz, respectively. The ^{31}P chemical shifts are referred to 85 % H_3PO_4, and the ^{13}C and ^{1}H chemical shifts are referred to TMS. The couplings are given in Hz. Melting point of **3a** was determined using a Bibby Scientific SMP10 Melting Point Apparatus. The exact mass measurements were performed using an Agilent 6545 Q-TOF mass spectrometer in high resolution, positive electrospray mode.

General procedure for the P–C coupling of bromobenzene and diphenylphosphine oxide in the presence of Ni(II) salts

To 0.052 mL (0.50 mmol) of bromobenzene was added diphenylphosphine oxide [0.10 g (0.50 mmol) or 0.11 g (0.55 mmol) or 0.12 g (0.60 mmol) or 0.13 g (0.65 mmol)], 0.16 g (0.50 mmol) of cesium carbonate, 0.0065 g

(0.050 mmol) of nickel chloride or 0.011 g (0.050 mmol) of nickel bromide and 1 mL of acetonitrile, and the resulting mixture was irradiated in a CEM Discover type MW reactor for the time shown in Table 1. The crude product was filtrated. The crude reaction mixture was analyzed by ^{31}P NMR spectroscopy and purified with column chromatography using silica gel and ethyl-acetate – hexane as the eluent. Product **3a** was obtained as white crystals in purity of >99 %. See the Supporting Information for the characterization and spectroscopic data of compound **3a**.

General procedure for the P–C coupling of bromobenzene and diethyl phosphite in the presence of Ni(II) salts

To 0.11 mL (1.0 mmol) of bromobenzene was added 0.15 mL (1.2 mmol) of diethyl phosphite, 0.14 g (1.0 mmol) of potassium carbonate, 0.013 g (0.10 mmol) of nickel chloride or 0.022 g (0.10 mmol) of nickel bromide and 1 mL of acetonitrile, and the resulting mixture was irradiated in a CEM Discover type MW reactor for the time shown in Table 1. The crude product was filtrated and purified with column chromatography using silica gel and ethyl-acetate – hexane as the eluent. Product **3b** was obtained as colorless oil in purity of >99 %. See the Supporting Information for the characterization and spectroscopic data of compound **3b**.

Theoretical calculations

All computations were carried out with the Gaussian09 program package (G09) [39], using convergence criteria of 3.0×10^{-4}, 4.5×10^{-4}, 1.2×10^{-3} and 1.8×10^{-3}, for the gradients of the root mean square (RMS) Force, Maximum Force, RMS displacement and maximum displacement vectors, respectively. Computations were carried out at B3LYP level of theory [40], using the 6-31G(d,p) basis set. The vibrational frequencies were computed at the same levels of theory, in order to confirm properly all structures as residing at minima on their potential energy hypersurfaces (PESs). Thermodynamic functions *U*, *H*, *G* and *S* were computed at 298.15 K. Beside the vacuum calculations, the IEFPCM method was also applied to model the solvent effect, by using the default settings of G09, modelling MeCN solvent [41]. For more precise calculations, in the acid base reactions, the explicit-implicit solvent model was used [42]. See the Supporting Information for details.

Acknowledgments: This project was sponsored by the National Research, Development and Innovation Office (K119202) and by the ÚNKP-19-3 New National Excellence Program of the Ministry for the Innovation and Technology. R. Henyecz is grateful for the support of the Gedeon Richter's Talentum Foundation.

References

[1] T. Hirao, T. Masunaga, Y. Ohshiro, T. Agawa. *Tetrahedron Lett.* **21**, 3595 (1980).
[2] T. Hirao, T. Masunaga, N. Yamada, Y. Ohshiro, T. Agawa. *Bull. Chem. Soc. Jpn.* **55**, 909 (1982).
[3] E. Jablonkai, G. Keglevich. *Curr. Org. Synth.* **11**, 429 (2014).
[4] E. Jablonkai, G. Keglevich. *Curr. Green Chem.* **2**, 379 (2015).
[5] M. Kalek, J. Stawinski. *Organometallics* **26**, 5840 (2007).
[6] E. L. Deal, C. Petit, J.-L. Montchamp. *Org. Lett.* **13**, 3270 (2011).
[7] O. Berger, C. Petit, E. L. Deal, J.-L. Montchamp. *Adv. Synth. Catal.* **355**, 1361 (2013).
[8] E. Jablonkai, G. Keglevich. *Tetrahedron Lett.* **54**, 4185 (2013).
[9] G. Keglevich, E. Jablonkai, L. B. Balázs. *RSC Adv.* **4**, 22808 (2014).
[10] G. Keglevich, R. Henyecz, Z. Mucsi, N. Z. Kiss. *Adv. Synth. Catal.* **359**, 4322 (2017).
[11] R. Henyecz, Z. Mucsi, G. Keglevich. *Pure Appl. Chem.* **91**, 121 (2019).
[12] C. Shen, G. Yang, W. Zhang. *Org. Biomol. Chem.* **10**, 3500 (2012).
[13] X. Zhang, H. Liu, X. Hu, G. Tang, J. Zhu, Y. Zhao. *Org. Lett.* **13**, 3478 (2011).
[14] S. Gong, Y.-L. Chang, K. Wu, R. White, Z.-H. Lu, D. Song, C. Yang. *Chem. Mater.* **26**, 1463 (2014).
[15] L. Wang, B. Pan, L. Zhu, B. Wang, Y. Wang, Y. Liu, J. Jin, J. Chen, D. Ma. *Dyes Pigments* **114**, 222 (2015).

[16] B. Pan, H. Huang, X. Yang, J. Jin, S. Zhuang, G. Mua, L. Wang. *J. Mater. Chem. C* **2**, 7428 (2014).
[17] B. Wang, X. Lv, B. Pan, J. Tan, J. Jin, L. Wang. *J. Mater. Chem. C* **3**, 11192 (2015).
[18] L. Liu, Y. Wang, Z. Zeng, P. Xu, Y. Gao, Y. Yin, Y. Zhao. *Adv. Synth. Catal*. **355**, 659 (2013).
[19] A. Kinbara, M. Ito, T. Abe, T. Yamagishi. *Tetrahedron* **71**, 7614 (2015).
[20] G. Hu, W. Chen, T. Fu, Z. Peng, H. Qiao, Y. Gao, Y. Zhao. *Org. Lett*. **15**, 5362 (2013).
[21] J. Xuan, T.-T. Zeng, J.-R. Chen, L.-Q. Lu, W.-J. Xiao. *Chem. Eur. J*. **21**, 1 (2015).
[22] L.-L. Liao, Y.-Y. Gui, X.-B. Zhang, G. Shen, H.-D. Liu, W.-J. Zhou, J. Li, D.-G. Yu. *Org. Lett*. **19**, 3735 (2017).
[23] J.-S. Zhang, T. Chen, J. Yanga, L.-B. Han. *Chem. Commun*. **51**, 7540 (2015).
[24] I. P. Beletskaya, E. G. Neganova, Y. A. Veits. *Russ. J. Org. Chem*. **40**, 1782 (2004).
[25] H.-Y. Zhang, M. Sun, Y.-N. Ma, Q.-P. Tian, S.-D. Yang. *Org. Biomol. Chem*. **10**, 9627 (2012).
[26] Y.-L. Zhao, G.-J. Wu, F.-S. Han. *Chem. Commun*. **48**, 5868 (2012).
[27] Y.-L. Zhao, G.-J. Wu, Y. Li, L.-X. Gao, F.-S. Han. *Chem. Eur. J*. **18**, 9622 (2012).
[28] J.-F. Wen, W. Hong, K. Yuan, T. C. W. Mak, H. N. C. Wong. *J. Org. Chem. **68***, 8918 (2003).
[29] D. Cai, J. F. Payack, D. R. Bender, D. L. Hughes, T. R. Verhoeven, P. J. Reider. *J. Org. Chem*. **59**, 7180 (1994).
[30] S. Gladiali, R. Taras, R. M. Ceder, M. Rocamora, G. Muller, X. Solans, M. Font-Bardia. *Tetrahedron: Asymmetry* **15**, 1477 (2004).
[31] C. Liu, M. Szostak. *Angew. Chem. Int. Ed*. **56**, 12718 (2017).
[32] Y. Wu, L. Liu, K. Yan, P. Xu, Y. Gao, Y. Zhao. *J. Org. Chem*. **79**, 8118 (2014).
[33] J. Yang, J. Xiao, T. Chen, L.-B. Han. *J. Organomet. Chem*. **820**, 120 (2016).
[34] J. Yang, T. Chen, L.-B. Han. *J. Am. Chem. Soc*. **137**, 1782 (2015).
[35] J. Yang, J. Xiao, T. Chen, L.-B. Han. *J. Org. Chem*. **81**, 3911 (2016).
[36] J. Yang, J. Xiao, T. Chen, S.-F. Yin, L.-B. Han. *Chem. Commun*. **52**, 12233 (2016).
[37] E. Łastawiecka, A. Flis, M. Stankevič, M. Greluk, G. Słowik, W. Gac. *Org. Chem. Front*. **5**, 2079 (2018).
[38] E. Jablonkai, L. B. Balázs, G. Keglevich. *Curr. Org. Chem*. **19**, 197 (2015).
[39] M. J. Frisch, G. W. Trucks, H. B. Schlegel, G. E. Scuseria, M. A. Robb, J. R. Cheeseman, G. Scalmani, V. Barone, B. Mennucci, G. A. Petersson, H. Nakatsuji, M. Caricato, X. Li, H. P. Hratchian, A. F. Izmaylov, J. Bloino, G. Zheng, J. L. Sonnenberg, M. Hada, M. Ehara, K. Toyota, R. Fukuda, J. Hasegawa, M. Ishida, T. Nakajima, Y. Honda, O. Kitao, H. Nakai, T. Vreven, J. A. Montgomery Jr, J. E. Peralta, F. Ogliaro, M. Bearpark, J. J. Heyd, E. Brothers, K. N. Kudin, V. N. Staroverov, R. Kobayashi, J. Normand, K. Raghavachari, A. Rendell, J. C. Burant, S. S. Iyengar, J. Tomasi, M. Cossi, N. Rega, J. M. Millam, M. Klene, J. E. Knox, J. B. Cross, V. Bakken, C. Adamo, J. Jaramillo, R. Gomperts, R. E. Stratmann, O. Yazyev, A. J. Austin, R. Cammi, C. Pomelli, J. W. Ochterski, R. L. Martin, K. Morokuma, V. G. Zakrzewski, G. A. Voth, P. Salvador, J. J. Dannenberg, S. Dapprich, A. D. Daniels, O. Farkas, J. B. Foresman, J. V. Ortiz, J. Cioslowski, D. J. Fox. *Gaussian 09, Revision A.1*, Gaussian, Inc., Wallingford, CT (2009).
[40] A. D. Beke. *J. Chem. Phys*. **98**, 5648 (1993).
[41] J. Tomasi, B. Mennucci, R. Cammi. *Chem. Rev*. **105**, 2999 (2005).
[42] Z. Mucsi, A. Szabo, I. Hermecz, A. Kucsman, I. G. Csizmadia. *J. Am. Chem. Soc*. **127**, 7615 (2005).
[43] Y. Li, L. Zou, R. Bai, Y. Lan. *Org. Chem. Front*. **5**, 615 (2018).
[44] G. Keglevich, N. Z. Kiss, Z. Mucsi, T. Körtvélyesi. *Org. Biomol. Chem*. **10**, 2011 (2012).
[45] N. Z. Kiss, Z. Mucsi, É. Böttger, L. Drahos, G. Keglevich. *Curr. Org. Synth*. **11**, 767 (2014).
[46] G. Keglevich, Z. Mucsi. in *Microwave Chemistry*, G. Cravotto, D. Carnaroglio, (Eds.), pp. 53–64, De Gruyter, Berlin (2017).
[47] G. Keglevich, N. Z. Kiss, Z. Mucsi. *Pure Appl. Chem*. **88**, 931 (2016).
[48] B. L. Hayes. *Microwave Synthesis – Chemistry at the Speed of Light*, p. 23, CEM Publishing, Matthews (2002).

Supplementary Material: The online version of this article offers supplementary material (https://doi.org/10.1515/pac-2019-1004).